In situ Monitoring of Solid Fat Content by Means of Pulsed Nuclear Magnetic Resonance Spectrometry and Ultrasonics

Silvana Martini[a], Constantin Bertoli[b], Maria Lidia Herrera[c], Ian Neeson[d], and Alejandro Marangoni[a,*]

[a]Department of Food Science, University of Guelph, Guelph, Ontario, Canada, [b]Nestlé Research Centre, Lausanne, Switzerland, [c]Departamento de Industrias, Facultad de Ciencias Exactas y Naturales, University of Buenes Aires, Argentina, and [d]VN Instruments Ltd., Elizabethtown, Ontario, Canada

ABSTRACT: An ultrasonic technique was developed to study the crystallization process of edible fats on-line. A chirp wave was used instead of the conventional pulser signal, thus achieving a higher signal-to-noise ratio. This enabled measurements to be made in concentrated systems [~20% solid fat content (SFC)] through a 8.11-cm thick sample without significant signal loss. Fat samples were crystallized at 20, 25, and 30°C at a constant agitation rate of 400 rpm for 90 min. The crystallization process was followed by ultrasonic spectroscopy and a low-resolution pulsed nuclear magnetic resonance spectrometer. Specific relationships were found between ultrasonic parameters [integrated response, time of flight (TF), and full width half maximum] and SFC. TF, which is an indirect measurement of the ultrasonic velocity (v), was highly correlated to SFC ($r^2 > 0.9$) in a linear fashion (v = 2.601 SFC + 1433.0).

Paper no. J10957 in *JAOCS 82*, 305–312 (May 2005).

KEY WORDS: Full width half maximum, integrated response, p-NMR, solid fat content, time of flight, ultrasonic velocity.

Sensing and measurement of food properties is crucial to the improvement of the quality of food and profitability of food manufacturing operations. Instrumental measurements can reduce the dependence on time-consuming chemical and sensory analysis. Measurements should provide some information about the food (e.g., temperature, composition, structure, concentration) that will be useful in controlling final product quality. The response time is crucial, so although laboratory tests on finished product are valuable, measurements made on-line of the freshly made or in-process foods are better. On-line sensors used in the food industry must also be inexpensive and robust to survive in the frequently hot and wet environment of a food-processing plant. The technique should also be both nondestructive and amenable to hygienic design principles (ideally, noninvasive). It should also provide a relatively simple output to an operator or an automated control system (1).

Ultrasonic technology has advantages over many techniques because it can be applied to systems that are optically opaque, concentrated, and electrically nonconducting. In addition, ultrasonic measurements are rapid and precise, are nondestructive and noninvasive, can be fully automated, are nonhazardous, and are particularly suitable for on-line monitoring.

Ultrasound techniques exploit the interaction of high-frequency sound with matter to generate information about material physicochemical properties. Such techniques have been established and used in numerous fields such as medicine, oceanography, and materials science. A number of publications have demonstrated the usefulness of ultrasound in food research, including particle size determination, creaming, crystallization, and aggregation phenomena in emulsions (2,3). Ultrasound also has been used to characterize the rheological behavior of solid fat dispersions and xanthan/sucrose mixtures (4,5) and to calculate the percentage of frozen material in foods (6). The ultrasonic velocity of a fatty material increases as its solid fat content (SFC) increases; hence, ultrasonic velocity measurements can be used to determine SFC of emulsions and bulk fats (7–13). Previous work with solid/liquid fat measurements using ultrasonics has been successful at fat contents below 10%. Most of the trouble was related to problems getting a signal through the material, resulting in a high attenuation at SFC contents higher than 10% (11). Singh *et al*. (13) found a linear correlation between ultrasonic velocity and SFC for concentrated fat samples (~20% SFC) when they were crystallized in a 1.6-cm cell. These experiments were generally done with a simple pulser receiver combination and an oscilloscope. A new ultrasonic technology used in this study consisted in the generation of a chirp wave, instead of a traditional pulser, with low-frequency contact transducers. This system has a far greater dynamic range and capability, enabling the penetration of the ultrasonic signal through 8.11 cm of crystallized fat with high SFC values. As a result of its high penetration capacity, this new technology could be used for on-line measurements.

The objective of this work was to use this ultrasonic technology to explore relationships between ultrasonic parameters (integrated response, time of flight or velocity, and full width half maximum) and SFC determined by low-resolution pulsed nuclear magnetic resonance (p-NMR). Since there is a great need to determine SFC on-line in food processing operations, such a technique would lead to significant improvements in process control and product quality.

The third author is an associate researcher of the National Research Council of Argentina (CONICET).

*To whom correspondence should be addressed at Department of Food Science, University of Guelph, Guelph, Ontario, Canada, N1G 2W1.
E-mail: amarango@uoguelph.ca

MATERIALS AND METHODS

Crystallization procedure. Five fat samples (samples 1, 2, 3, 4, and 5 with melting points of 46.1, 43.5, 40.7, 41.2, and 36.6°C, respectively) were crystallized at 20, 25, and 30°C in a crystallization cell especially designed to monitor fat crystallization on-line by means of ultrasonic technology. Crystallization was performed under agitation using 400 rpm of shear. The agitation rate was constant for all samples and all crystallization temperatures to avoid variation in the ultrasonic measurement due to different shear rates. The cell temperature was controlled by means of water circulated from a water bath set at the particular crystallization temperature. Samples were heated to 120°C in an oven, held at this temperature for 30 min, and then introduced into the cell. The temperature profile was monitored by means of a thermocouple dipped into the sample, and the crystallization process was followed by means of ultrasonics and p-NMR for 90 min.

Chemical composition. The FA composition was determined using GC. A column of 5 mm outer diameter, 3 mm internal diameter, and 1.5 m long was filled with 10% Silar 9CP on Chromosorb W, AW 80/100 mesh (Chromatographic Specialties, Ltd., Brockville, Ontario, Canada). This column was placed in a gas–liquid chromatograph (model GC-8A; Shimadzu, Kyoto, Japan). The chromatograph oven was set at 60°C, and then a temperature ramp was programmed from 60 to 210°C at 8°C/min. The detector and injector temperatures were held at 230°C. Nitrogen was used as the carrier gas, and both hydrogen and air were used to feed the FID. Before chromatographic analysis, the FAME of the TAG FA were synthesized. A 50-mg sample of fat was placed in a vial and dissolved in 2 mL of iso-octane. KOH, 2 N in MeOH (200 μL), was added. The mixtures were vortexed for 1 min, and after 5 min, 2 drops of methyl orange were added. Finally, the sample was titrated with 2 N HCl until a pink end point was observed. Then 0.5 μL of the organic phase was injected into the chromatograph. The resulting peaks were integrated using a Shimadzu integrator (C-R3A Chromatopac). The chemical composition of the samples is detailed in Table 1.

Melting points. Melting points of the five fat samples were determined by means of DSC (model DSC 2910; DuPont Instruments). First, 5–10 mg of each melted sample was placed in an aluminum DSC pan. After placing the DSC pan in the DSC oven, it was heated at 10°C/min to 80°C and kept at this temperature for 15 min to ensure that the sample was completely melted. After this step, the sample was cooled at 10°C/min to 0°C and held at this temperature for another 15 min to induce crystallization. After this temperature cycle, the DSC pan was heated at 5°C/min to 80°C to follow the melting profile of the fats. The m.p. of the samples were reported as the peak temperature obtained from the melting thermograms. A thermal description (peak temperature, T_p; onset temperature, T_o; and final temperature, T_f) of the samples can be found in Table 2. Data reported in this work were the average of two independent runs.

Crystallization cell. The crystallization cell used to study the relationship between SFC and ultrasonic parameters is shown in Figure 1. This figure shows the two transducers from the ultrasonic spectrometer operating in contact mode (no air between the transducers and the sample). The crystallization cell was designed with two polycarbonate windows where the transducers were placed. Windows were made of polycarbonate since this material does not affect ultrasonic wave propagation. A good contact between the transducers and the windows was achieved by means of vacuum grease. Both transducers were aligned so that one of the transducers generated the ultrasonic wave and the other one received it (transmission mode). The wave propagation direction is indicated in Figure 1 by the arrow.

Ultrasonic measurements. Ultrasonic measurements were performed by means of an SIA-7 ultrasonic spectrometer (VN Instruments Ltd., Elizabethtown, Ontario, Canada). Transducers of 550 kHz and 1 MHz center frequency (GE Panametrics, Waltham, MA) were used to generate the ultrasonic wave. A chirp pulse was used in these experiments instead of the traditional pulser signal. The chirp pulse was generated over a range of frequencies with different amplitudes. The center frequency of the chirp corresponds to the transducer center frequency (550 kHz and 1 MHz), and the range of frequencies in which these transducers operate is called the bandwidth. A synthetic impulse (SI) was generated from the chirp by means of a digital receiver processor. Three parameters can be measured from the SI image: integrated response (IR), time of flight (TF), and full width half maximum (FWHM). The meaning of these parameters and how they are calculated will be described in the Results and Discussion section. Data reported are averages of two replicates.

TABLE 1
FA Composition (%) of the Five Samples Assayed

	Sample					
Carbon number	1	2	3	4	5	Canola oil
12:0	0.36	0.37	0.32	0.27	0.15	0
14:0	0.69	0.642	0.75	0.71	0.64	0.16
16:0	25.13	24.19	25.91	28.48	25.34	6.01
18:0	14.45	10.67	5.65	6.47	4.15	3.49
18:1	46.02	49.94	55.35	51.72	54.41	59.39
18:2	9.63	10.30	8.25	8.80	11.71	20.28
18:3 + 20:0	3.72	3.89	3.76	3.55	3.67	10.75
Total	100	100	100	100	100.08	100.08

TABLE 2
Thermal Parameters of the DSC Experiments Performed to Determine the m.p. of the Samples

DSC parameters[a]	Sample				
(°C)	1	2	3	4	5
T_o	30.9	28.6	18.6	26.1	29.3
T_p	46.1	43.5	40.7	41.2	36.6
T_f	52.6	49.6	46.3	46.7	44.1

[a]T_o, onset temperature; T_p, peak temperature; T_f, final temperature.

SFC measurements. SFC was measured by means of p-NMR (Bruker Optics Ltd., Milton, Ontario, Canada) as crystallization took place. Samples were taken from the crystallization cell with a Pasteur pipette and put into a NMR tube to perform the measurement. The crystallization process was followed by taking samples every minute for the first 10 min and then every 5 min until the end of crystallization process (90 min). Data reported are averages of two individual measurements. The error in the SFC determinations was approximately 1%.

Statistical analysis. Statistic analysis was performed to evaluate significant differences of the treatments using a one-way ANOVA test ($P < 0.05$).

RESULTS AND DISCUSSION

Ultrasonic measurements. The technology used in these experiments relies on the generation of a chirp wave instead of a pulser signal. The chirp wave contains a range of frequencies with different amplitudes. This signal starts at low frequency and amplitude and increases in frequency over the duration of the signal. Meanwhile, the amplitude reaches a maximum and then decreases. Therefore, these transducers operate over a range of frequencies (bandwidth) with a center frequency called transducer frequency (550 kHz and 1 MHz). A typical chirp wave is shown in Figure 2a. Chirp parameters (bandwidth and frequency) can be changed to obtain reliable data and an optimal signal-to-noise ratio. Both parameters are determined by the type of transducer used. The chirp generated by one of the transducers travels through the sample to reach the second transducer. Once the chirp wave has reached the second transducer (modified or not by the sample), it is processed by a digital receiver that converts this complicated signal into a simpler one. A digital receiver converts a waveform (such as a voice recorder or music) into a representation in which one sees the amplitude and phase of the data relative to an arbitrary reference signal that is predetermined. That is, a digital receiver converts raw data from zero frequency to a representation where the zero is shifted to $f = f_0$. The important thing to know about this procedure is that the digital receiver will provide an envelope of the signal while preserving the phase. This processed data, or envelope, is called the synthetic impulse (SI, Fig. 2b). The SI image contains all the necessary information to analyze the ultrasonic characteristics of a test sample. The advantages of SI over a standard pulser include a greatly improved signal-to-noise ratio, which can be achieved by increasing the duration of the chirp signal and by increasing its amplitude. The SI signal is characterized by three parameters: IR (area under the curve), TF (position of the peak), and FWHM (width of the peak).

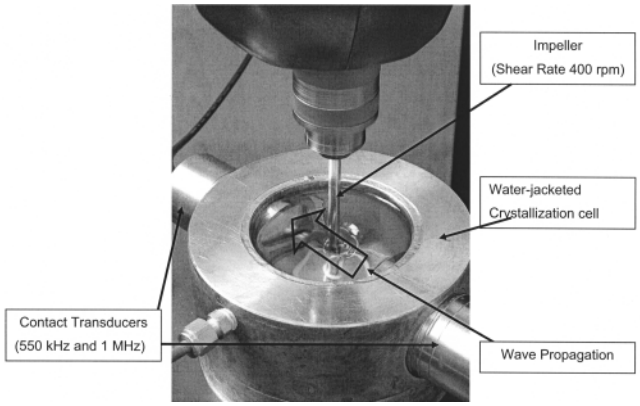

FIG. 1. Crystallization cell especially designed to monitor the crystallization process on-line of fat samples by means of ultrasonic technology.

(i) IR. This parameter measures the power needed to go through a sample. Therefore, the IR is a direct measurement of the attenuation of the signal. As an ultrasonic wave travels through a material, it is attenuated, i.e., its amplitude decreases with distance traveled. The major causes of attenuation are absorption and scattering. Absorption occurs to some extent in all materials as a result of the thermodynamic relaxation mechanisms that convert energy from the ultrasonic wave into some other form, ultimately heat (12). Scattering is often the predominant form of attenuation in heterogeneous materials. It occurs when some of the ultrasonic wave incident on a discontinuity in a material (e.g., a particle) is scattered in a direction that is different from that of the incident wave. Scattering of ultrasound is important in many systems since it can have a significant effect on measured ultrasonic properties, making the velocity and attenuation dependent on particle size as well as concentration.

(ii) TF. The TF depends on the time it takes for the wave to go from one transducer to the other. If we place a sample between the transducers, it will displace some air and, since the speed of sound in the test sample is usually different from the speed of sound in air, the position of the peak, or TF, will change in accordance with the change of velocity. The distance traveled is a constant (8.11 cm), and it depends on the cell geometry. This distance can be calculated by measuring the TF of distilled water, for which the velocity is a known constant (1482.3 m/s at 20°C). Therefore, as velocity is distance traveled, 8.11 cm in our experimental conditions, in a period of time (TF), we can express our results in function of velocity ($v = 8.11/TF$).

(iii) FWHM. The FWHM measures the width of the SI peak at half its amplitude and is an estimate of the time resolution of the system. The time resolution of this SI is the width of the curve. If two signals are present in an image, we would require that the signals be distinct enough to tell them apart. If they are too close together, the "overlap" creates ambiguity. For an SI,

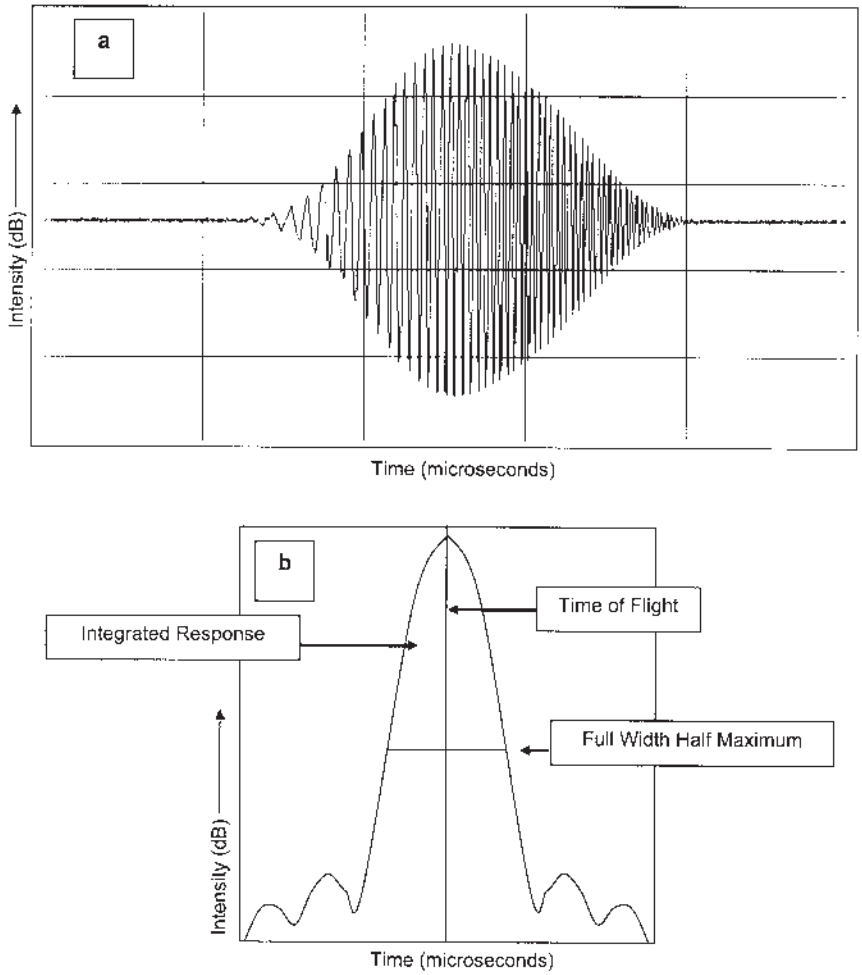

FIG. 2. Typical chirp wave (a) and synthetic impulse (b) generated by the transducers.

the FWHM is expressed in microseconds and is a good indicator of the time resolution of the system. The greater the FWHM value, the wider the peak, and therefore, the worse the resolution of the system. This parameter is determined almost entirely by the bandwidth of the transducers and the shape of the chirp used to drive them. In general, larger bandwidths (generated by transducers of higher frequencies) produce smaller FWHM values and therefore a better time resolution.

Variation of ultrasonic parameters with time. The ultrasonic parameters, IR, velocity (v), and FWHM were used to follow the crystallization process of samples 1, 2, 3, 4, and 5 at 20, 25, and 30°C. Canola oil was also studied in order to know how these parameters behave when no crystallization occurs, since oil does not crystallize at the temperatures used. These parameters were measured with 550 kHz and 1 MHz transducers. Figure 3 shows the variation of IR, v, and FWHM values measured with 550 kHz and 1 MHz transducers for all the samples crystallized at 25°C. Figures 3a and 3b show that the IR values increased while the sample temperature decreased toward the final crystallization temperature (first 3 min of the crystallization process approximately). This behavior was observed for all samples crystallized at all crystallization temperatures assayed and with both transducers. When the crystallization temperature was reached, the IR value remained constant until the onset of crystallization. We can appreciate, for example, that this parameter remained constant for canola oil for the duration of the experiment (90 min) since no crystallization took place in this sample. For samples 1–5, when crystallization started, the IR value decreased, showing attenuation of the ultrasonic signal. This means that the ultrasonic signal generated by the first transducer could not completely reach the second one because it had been partially scattered by the solid fat. The decrease in the IR value was in accordance with the induction times of crystallization of each sample. This means that for samples that were more supercooled, as for example in sample 1, with a m.p. of 46.1°C, the IR decreased before sample 4 crystallized at the same temperature. The latter has a lower m.p. (41.2°C) and therefore is less supercooled, needing more time to crystallize. Once crystallization started, the IR values became more attenuated as the crystallization process continued and, in some cases, the signal was totally attenuated by the solid (for example, sample 3 crystallized at 25 with 550 kHz and 1 MHz, Figs. 3a and 3b). Comparing the measurements made with different transducers (Figs. 3a and 3b), we can ap-

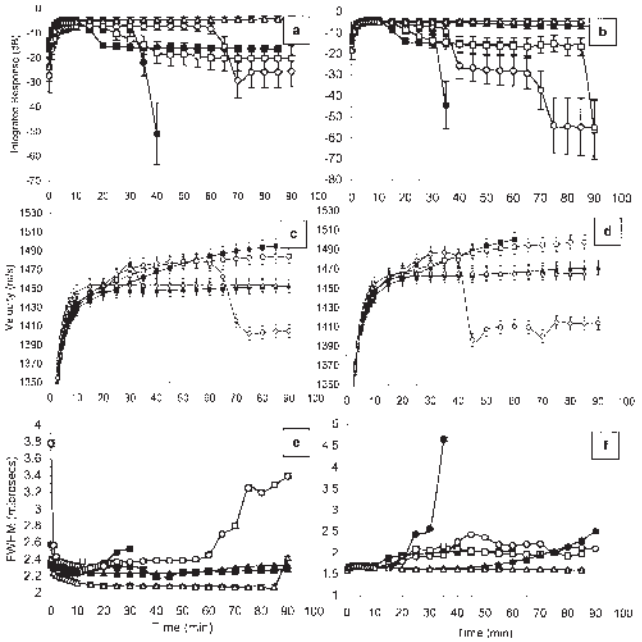

FIG. 3. Integrated response (IR), velocity, and full width half maximum (FWHM) values vs. time for all samples crystallized at 25°C with 550 kHz (a, c, and e, respectively) and 1 MHz transducers (b, d, and f, respectively). ■, □, ●, ○, ▲, and △ for samples 1, 2, 3, 4, 5, and canola oil, respectively.

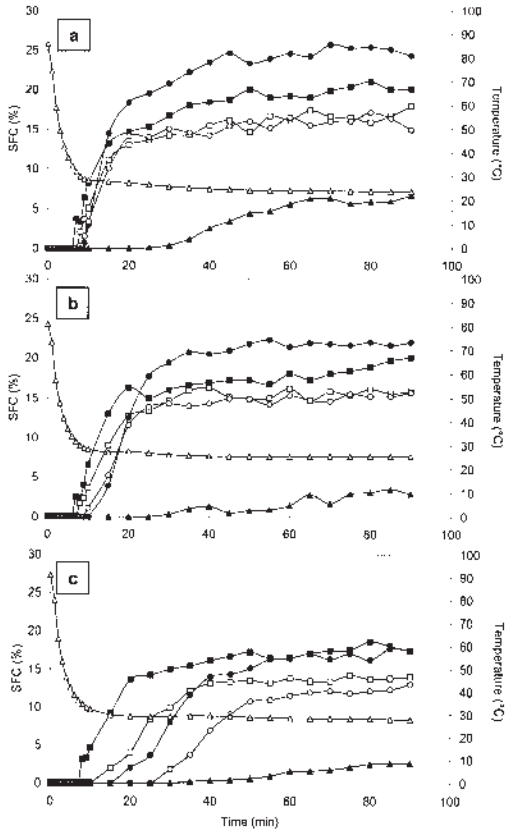

FIG. 4. Solid fat content (SFC) variation during the crystallization process determined by means of pulsed NMR (p-NMR). ■, □, ●, ○, and ▲ for samples 1, 2, 3, 4, and 5, respectively, crystallized at 20 (a), 25 (b), and 30°C (c). The temperature profile for each temperature is shown (△).

preciate that samples 2 and 4 displayed complete attenuation when the measurements were made with the 1 MHz transducer but only partial attenuation when the measurements were made with the 550 kHz transducers. The same behavior was observed for sample 4 crystallized at 30°C (data not shown). These behaviors suggest that the 1 MHz transducer was more sensitive to attenuation than the one at 550 kHz.

The ultrasonic velocity, v, increased as the sample temperature decreased to reach the crystallization temperature (Figs. 3c and 3d). When the samples reached the crystallization temperature, v values remained constant until crystallization started, showing at this point a slight change in the slope of the curve. When crystallization was almost complete, the velocity decreased as a result of the attenuation. When the ultrasonic signal is attenuated, the SI peak becomes smaller and broader and therefore the determination of the TF is not very accurate. As described for the variation of IR upon crystallization, the v inflection point was in accordance with the onset of crystallization of the different samples at different temperatures. That is, changes in v values were observed at shorter times for samples showing shorter induction times owing to a higher supercooling effect. Once the sample had reached the onset of crystallization, v increased as the crystallization process continued. This is an expected result since ultrasonic velocity is higher in a solid than in a liquid phase. We can appreciate the v behavior in the absence of crystallization by observing the canola oil plot.

FWHM values decreased with decreasing sample temperature (Figs. 3e and 3f). On reaching the set crystallization temperature, the FWHM remained constant until crystallization started. If no crystallization was observed (as, for example, in canola oil samples), the FWHM value remained constant. When crystallization took place, the FWHM increased according to the expected crystallization behavior of each sample at a specific temperature. The increase in FWHM values indicated that attenuation was changing as a function of frequency. This means that the higher-frequency components were scattered by the crystallized material; therefore, a narrower bandwidth was detected by the second transducer, resulting in a higher FWHM.

Data obtained from these experiments show that ultrasonic parameters can be used to monitor the crystallization process since these parameters change when crystallization occurs depending on the sample and the crystallization temperature used.

SFC determination. The SFC variation during the crystallization process was followed by means of p-NMR as described in the Materials and Methods section. As expected, SFC increased as crystallization took place. SFC variation with crystallization time for all samples crystallized at different temperatures is shown in Figure 4. The canola oil sample did not crystallize at any of the temperatures assayed and therefore its SFC was 0 during the experimental time.

Relationship between ultrasonic parameters and SFC. Figure 5 shows the IR behavior as SFC increases during crystal-

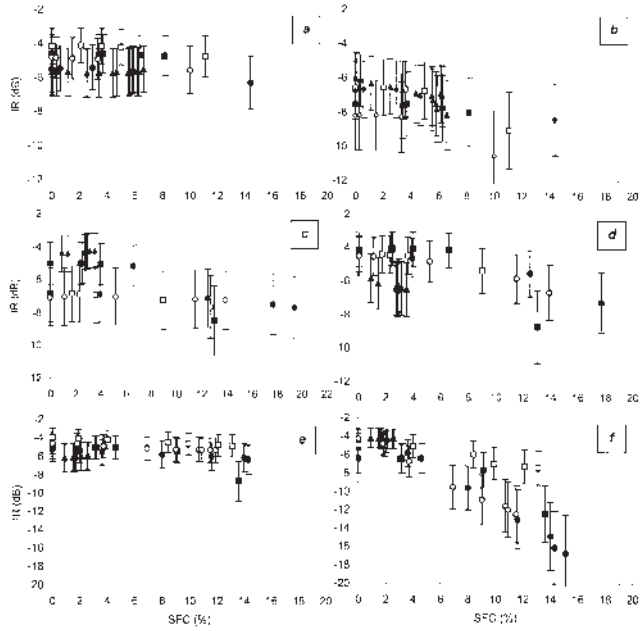

FIG. 5. IR variation with SFC for all samples crystallized at 20, 25, and 30°C with 550 kHz (a, c, and e, respectively) and 1 MHz transducers (b, d, and f, respectively). ■, □, ●, ○, and ▲ for samples 1, 2, 3, 4, and 5, respectively. For abbreviations see Figures 3 and 4.

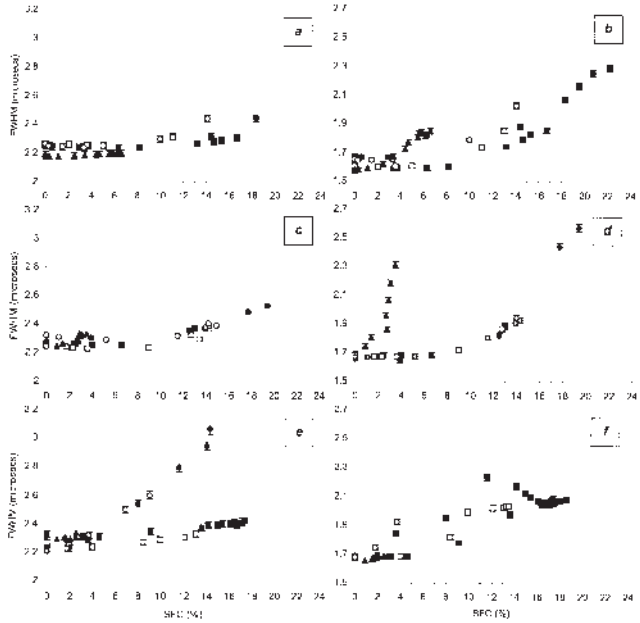

FIG. 6. FWHM variation with SFC for all samples crystallized at 20, 25, and 30°C with 550 kHz (a, c, and e, respectively) and 1 MHz transducers (b, d, and f, respectively). ■, □, ●, ○, and ▲ for samples 1, 2, 3, 4, and 5, respectively. For abbreviations see Figures 3 and 4.

lization for all samples crystallized at 20, 25, and 30°C when the measurements were made with 550 kHz and 1 MHz transducers. This figure shows that in most cases, IR decreases as SFC increases, which is an expected result due to the attenuation of the signal caused by the crystallized fat. The error in IR determinations was between 25 and 50%. Even though this is a high error for the absolute value of IR, the tendencies of the curves were quite reproducible. The differences found between the IR replicates can be explained by considering that the IR represents the power of the signal that passes through the sample. The absolute value of the power is very sensitive to the agitation rate, position of the impeller, flow lines in the liquid produced by shear, and so on. No matter which is the absolute value of the IR parameter, the variation of this value with temperature or between the liquid and crystallized fat is constant between replicates. IR and SFC were related in a nonlinear fashion. Small increases in SFC caused attenuation of the signal (for example, sample 1 in Fig. 5c and samples 1 and 4 in Fig. 5d) lead to a large decrease in IR. The attenuation seems to happen especially after the sample reaches ~8% of SFC, but it seems to be system dependent. These results are in accordance with the data reported by Singh *et al.* (10,13). This fact suggests that some other factors than the SFC might be affecting the attenuation of the signal.

Figure 6 shows the variation of FWHM with SFC for all samples crystallized at 20, 25, and 30°C and measured with 550 kHz and 1 MHz transducers, respectively. FWHM increases as SFC increases due to the change of attenuation as a function of frequency as described before. This figure shows the average data for two independent runs, with an error of ~1%. A nonlinear dependence between FWHM and SFC is observed. Significant differences between the measurements made with the 550 kHz and 1 MHz transducer can be appreciated from Figure 6; these were expected since FWHM is highly dependent on the bandwidth of the signal. Measurements made with 550 kHz transducers have a bandwidth of 650 kHz whereas 1 MHz transducers have a bandwidth of 900 kHz. Higher bandwidths, as is the case of the 1 MHz transducers, result in lower FWHM.

Figure 7 shows the variation of v with SFC for all samples crystallized at 20, 25, and 30°C with the different transducers. Data shown are the average of two independent runs, and the error is ~0.5%. As expected, v increased as SFC increased as a result of the difference in the ultrasonic velocity value between the liquid and the solid fat. Linear regression was used to fit the v vs. SFC data. The linear parameters of these lines (slope and *y*-intercept) were not significantly different from each other, and the regression coefficients were around 0.9 (Table 3). The correlation analysis was made using data points starting from the onset of crystallization (SFC ≠ 0). Also, data points that showed high attenuation were not taken into account for the linear regression analysis since, as explained before, when attenuation occurs the TF measurement is less accurate than when no attenuation is present. The same criterion was used for data shown in Figures 5 and 6.

ANOVA test. Analyzing the variation of the three ultrasonic parameters (IR, v, and FWHM) with SFC (Figs. 5–7 and Table 3), we can appreciate that the ultrasonic velocity is the one that best describes the crystallization behavior of the samples. Therefore, v was chosen to calculate the SFC of the samples by means of ultrasonic technology. The v vs. SFC of each sample can be

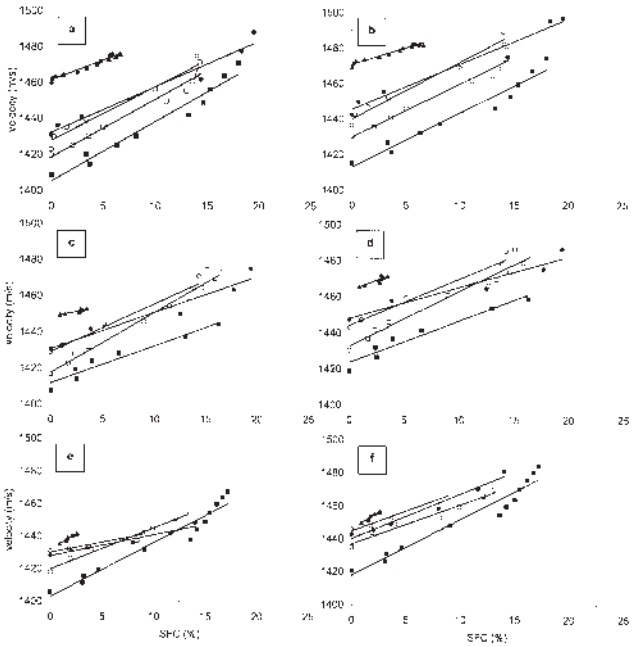

FIG. 7. Velocity variation with SFC for all samples crystallized at 20, 25, and 30°C with 550 kHz (a, c, and e, respectively) and 1 MHz transducers (b, d, and f, respectively). ■, □, ●, ○, and ▲ for samples 1, 2, 3, 4, and 5, respectively. For abbreviation see Figure 4.

predicted by the linear regression parameters described in Table 3. This means that by measuring the v of a specific sample at a chosen crystallization temperature (20, 25, or 30°C) using transducers of 550 kHz or 1 MHz of frequency, we can calculate its SFC. It is obvious from this statement that these regressions are system, temperature, and transducer specific.

To analyze whether the crystallization temperature and the transducers used to perform the experiment had an effect on the linear regression parameters found, a one-way ANOVA test was performed on the slope and *y*-intercept values of v vs. SFC data. No significant differences were found in these parameters between the crystallization temperature and transducers used. Taking these results into account, a unique equation can be derived describing the relationship between v and SFC. The global equation obtained is:

$$v = 2.601\ SFC + 1433.0 \quad [1]$$

The SE in the *y*-intercept is ±16.48 and in the slope is ±0.7160. However, a one-way ANOVA test of the slopes and the *y*-intercepts of Table 3, made to compare differences between samples, showed that they were significantly different. Therefore, Equation 1 is sample dependent, and more accurate results will be obtained if SFC is calculated with the particular equations shown in Table 3.

Figure 8 compares SFC values obtained using the ultrasonic technique (measuring TF, and therefore velocity) and the p-NMR method for samples crystallized at 25°C. The ultrasonic data were calculated using the particular correlation values of the specific linear regression of each sample crystallized at a

TABLE 3
Parameters of the Linear Fit Between the Ultrasonic Velocity (v) and the Solid Fat Content (SFC) Values for All Samples Crystallized at 20, 25, and 30°C for Measures Made with 550 kHz and 1 MHz Transducers

	Regression values (v = a + b SFC)					
	T_c = 20°C					
	550 kHz			1 MHz		
Sample	a	b	R^2	a	b	R^2
1	1405.1	3.2920	0.9631	1412.9	3.0540	0.9566
2	1418.4	3.2057	0.9653	1429.8	2.9944	0.9667
3	1432.0	2.5401	0.9650	1445.4	2.5514	0.9698
4	1427.6	2.9836	0.9588	1440.0	3.2037	0.9786
5	1461.4	2.2012	0.9701	1470.8	1.8639	0.9664
	T_c = 25°C					
	550 kHz			1 MHz		
Sample	a	b	R^2	a	b	R^2
1	1411.8	2.0454	0.9398	1423.7	2.2904	0.9454
2	1417.7	3.2828	0.9615	1432.7	3.0013	0.9654
3	1430.8	1.9748	0.9317	1447.9	1.7131	0.9222
4	1429.3	2.5902	0.9656	1444.1	2.5519	0.9616
5	1448.1	1.2106	0.7207	1463.2	2.3569	0.7813
	T_c = 30°C					
	550 kHz			1 MHz		
Sample	a	b	R^2	a	b	R^2
1	1402.8	3.3332	0.9480	1417.8	3.3964	0.9463
2	1419.8	2.5400	0.9742	1436.9	2.3777	0.9630
3	1427.9	1.3104	0.9550	1440.2	2.7025	0.9762
4	1430.1	1.2435	0.9646	1444.7	2.4269	0.9718
5	1432.2	3.6806	0.9250	1446.1	4.1117	0.9519

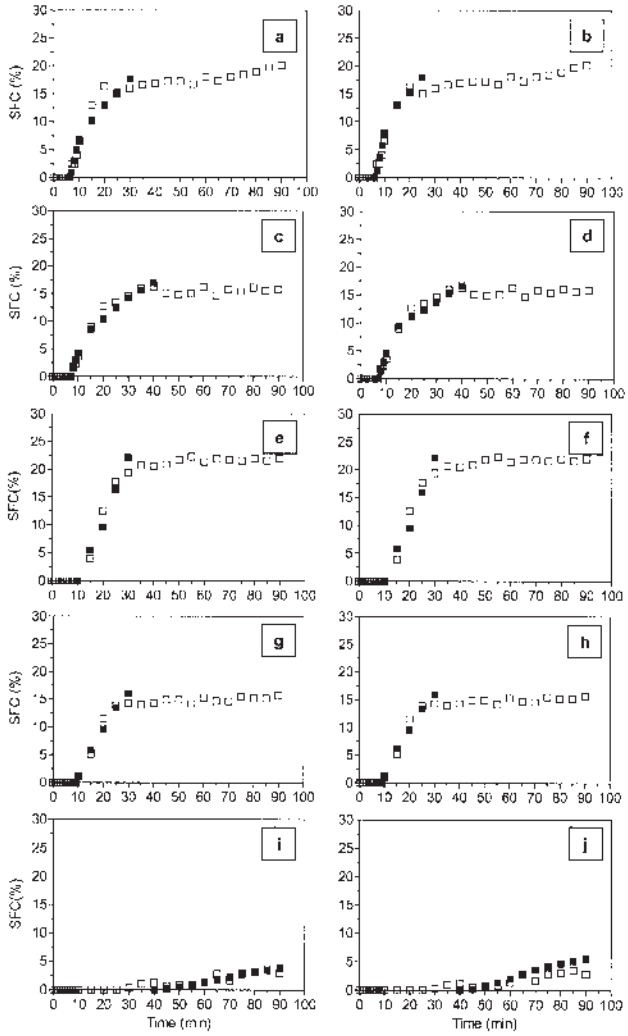

FIG. 8. Comparison between SFC values measured with p-NMR (□) and ultrasonics (■) for samples crystallized at 25°C. Sample 1 (a, b), sample 2 (c, d), sample 3 (e, f), sample 4 (g, h) and sample 5 (i, j) with 550 kHz and 1 MHz transducers, respectively. For abbreviations see Figure 4.

specific crystallization temperature and using a specific transducer (Table 3). These data show that no significant differences were found between the values obtained with the ultrasonic and the p-NMR methods. Therefore, we can use ultrasonic spectroscopy to determine SFC on-line accurately in a simple way. It is important to notice here that when the samples reached their plateau in the SFC curve, no measurements were possible using the ultrasonic technology owing to the high attenuation of the wave. However, the attenuation observed was not dependent only on the SFC of the sample. For example, we can appreciate in Figures 8a and 8b (sample 1) that the attenuation starts at approximately 17% whereas in Figures 8e and 8f (Sample 3) the attenuation starts at about 22%.

From the data reported in this work, we can reach several important conclusions. The crystallization process of fats can be monitored using ultrasonics. Specific relationships exist between the ultrasonic velocity and SFC that enable the measurement of SFC during crystallization in an 8-cm thick sample. Therefore, this new technology can be used to perform on-line measurements.

ACKNOWLEDGMENTS

The authors acknowledge the financial support of the Natural Sciences & Engineering Research Council of Canada (NSERC) and the Ontario Ministry of Food (OMAF). Dr. Martini thanks the National Research Council of Argentina (CONICET) for her postdoctoral fellowship.

REFERENCES

1. Coupland, J.N., and R. Saggin, Ultrasonic Sensing for the Food Industry, *Adv. Food Nutr. Res. 42*:102–166 (2003).
2. McClements, D.J., and M.J.W. Povey, Ultrasonic Analysis of Edible Fats and Oils, *Ultrasonics 30*:383–388 (1992).
3. McClements, D.J., M.J.W. Povey, and E. Dickinson, Absorption and Velocity Dispersion Due to Crystallization and Melting of Emulsion Droplets, *Ibid. 31*:433–437 (1993).
4. Saggin, R., and J.N. Coupland, Shear and Longitudinal Ultrasonic Measurements of Solid Fat Dispersions, *J. Am. Oil Chem. Soc. 81*:27–32 (2004).
5. Saggin, R., and J.N. Coupland, Rheology of Xanthan/Sucrose Mixtures at Ultrasonic Frequencies, *J. Food Eng. 65*:49–53 (2002).
6. Sigfusson, H., G.R. Ziegler, and J.N. Coupland, Ultrasonic Monitoring of Food Freezing, *Ibid. 62*:263–269 (2004).
7. Miles, C.A., G.A.J. Fursey, and R.C.D. Jones, Ultrasonic Estimation of Solid/Liquid Ratios in Fats, Oils and Adipose Tissue, *J. Sci. Food Agric. 36*:215–228 (1985).
8. McClements, D.J., and M.J.W. Povey, Comparison of Pulsed NMR and Ultrasonic Velocity Techniques for Determining Solid Fat Contents, *Int. J. Food Sci. Technol*. 23:159–170 (1988).
9. McClements, D.J., and M.J.W. Povey, Investigation of Phase Transitions in Glyceride/Paraffin Oil Mixtures Using Ultrasonics Velocity Measurement, *J. Am. Oil Chem. Soc. 65*:1791–1795 (1988).
10. Singh, A.P., D.J. McClements, and A.G. Marangoni, Comparison of Ultrasonic and Pulsed NMR Techniques for Determination of Solid Fat Content, *Ibid. 79*:431–437 (2002).
11. Saggin, R., and J.N. Coupland, Measurement of Solid Fat Content by Ultrasonic Reflectance in Model Systems and Chocolate, *Food Res. Intl. 35*:999–1005 (2002).
12. McClements, D.J., Ultrasonic Characterization of Emulsions and Suspensions, *Adv. Colloid Interface Sci. 37*:33–72 (1991).
13. Singh, A.P., D.J. McClements, and A.G. Marangoni, Solid Fat Content Determination by Ultrasonic Velocimetry, *Food Res. Intl. 37*:545–555 (2004).

[Received September 30, 2004; accepted April 19, 2005]